Novel Bayesian Additive Regression Tree Methodology for Flood Susceptibility Modeling

Janizadeh, Saeid; Vafakhah, Mehdi; Kapelan, Zoran; Dinan, Naghmeh Mobarghaee

DOI
10.1007/s11269-021-02972-7

Publication date
2021

Document Version
Accepted author manuscript

Published in
Water Resources Management

Citation (APA)
Janizadeh, S., Vafakhah, M., Kapelan, Z., & Dinan, N. M. (2021). Novel Bayesian Additive Regression Tree Methodology for Flood Susceptibility Modeling. *Water Resources Management*, *35*(13), 4621-4646. https://doi.org/10.1007/s11269-021-02972-7

Novel Bayesian Additive Regression Tree methodology for flood susceptibility modeling

Saeid Janizadeh[1], Mehdi Vafakhah[1*], Zoran Kapelan[2] and Naghmeh Mobarghaee Dinan[3]

[1-] Department of Watershed Management Engineering and Sciences, Faculty in Natural Resources and Marine Science, Tarbiat Modares University, Tehran, 14115-111 Iran, janizadehsaeid@modares.ac.ir

[1-] Department of Watershed Management Engineering and Sciences, Faculty in Natural Resources and Marine Science, Tarbiat Modares University, Tehran, 14115-111 Iran,* Correspond author: vafakha@modares.ac.ir

2-Department of Water Management, Delft University of Technology, Delft, The Netherlands, z.kapelan@tudelft.nl.

3- Department of Environmental Planning and Design, Environmental Sciences Research Institute, Shahid Beheshti University, 1983969411 Tehran, Iran. n_mobarghaee@sbu.ac.ir

Abstract

Identifying areas prone to flooding is a key step in flood risk management. The purpose of this study is to develop and present a novel flood susceptibility model based on Bayesian Additive Regression Tree (BART) methodology. The predictive performance of the new model is assessed via comparison with the Naïve Bayes (NB) and Random Forest (RF) based methods that were previously published in the literature. All models were tested on a real case study based in the Kan watershed in Iran. The following fifteen climatic and geo-environmental variables were used as inputs into all flood susceptibility models: altitude, aspect, slope, plan curvature, profile curvature, drainage density, distance from river distance from road, stream power index (SPI), topographic wetness index (TPI), topographic position index (TPI), curve number (CN), land use, lithology and rainfall. Based on the existing flood field survey and other information available for the analyzed area, a total of 118 flood locations were identified as potentially prone to flooding. The

data available were divided into two groups with 70% used for training and 30% for validation of all models. The receiver operating characteristic (ROC) curve parameters were used to evaluate the predictive accuracy of the new and existing models. Based on the area under curve (AUC) the new BART (86%) model outperformed the NB (80%) and RF (85%) models. Regarding the importance of input variables, the results obtained showed that the location's altitude and distance from the river are the most important variables for assessing flooding susceptibility.

Keywords: Flood susceptibility mapping; Bayesian; Regression Tree; Ensemble model; Bayesian Additive Regression Tree (BART);

1. Introduction

Any unforeseen natural occurrence that weakens or destroys economic, social and physical capacity, such as loss of life and finances, destruction of infrastructure, economic resources and areas of employment is defined as a natural disaster. Examples include earthquakes, floods, drought, seawater, volcanoes, landslides, hurricanes and natural pests (Vetrivel et al. 2018). Flooding is one of the most dynamic and disruptive natural events that puts human life and property and social and economic conditions at greater risk than any other natural disaster (Rahmati et al. 2016; Yariyan et al. 2020). This phenomenon causes damage to human achievements at all times (Woodward et al. 2014; Darabi et al. 2019; Vafakhah et al. 2020). The highest risk of flooding and corresponding damage is in the populated, i.e. urban areas. In recent years, the increase in urban flood hazards, particularly along the river banks, has resulted in the risk of flooding for residents and movable property (Choubin et al. 2019). Due to the varying climate, unpredictable temperatures and rainfall in many of Iran's watersheds, several floods occur every year (Tehrany et al. 2014). Limiting environmental resources, reducing and destroying them as a result of the

46 expansion of human activities, poses many challenges for today's society and the next generation.
47 The Kan watershed is affected by flooding events annually and this vulnerability has been
48 documented (Hooshyaripor et al. 2020). Seven important flood events were recorded in this
49 watershed since …, causing damage to industrial, residential, agricultural land use, and fatalities,
50 according to the available information.

51 Reducing human casualties as well as damage to property and the environment is a key objective
52 shared by countries most often impacted by natural disasters. They are increasingly conducting
53 feasibility studies with economic analysis to mitigate the effects of these disasters (Molinos-
54 Senante et al. 2011). Although flooding cannot be prevented, the damage can be mitigated through
55 appropriate analysis and forecasting techniques (Heidari 2014). The first step is to identify flood-
56 prone areas (Janizadeh et al. 2019; Hosseini et al. 2020). One way to prevent and reduce flood
57 damage is to provide people with reliable information through flood hazard zoning maps (Cook
58 and Merwade 2009). The modelling of flood hazards, which may involve multi-temporal data sets,
59 is required. Recently, machine learning methods have been successfully applied to assess flood
60 risk with higher accuracy (Ngo et al. 2018; Talukdar et al. 2020). However, there is still no
61 agreement on which method or set of methods can provide the best predictions (Kalantar et al.
62 2021; Costache et al. 2021).

63 Rapid access to satellite imagery based on remote sensing data has increased the use of geographic
64 information systems in the preparation of flood susceptibility maps. A wide range of modelling
65 techniques has been proposed and used in natural disaster assessment including AI based
66 techniques (Sayers et al 2014). In recent years, Bayesian methods, partly because of their over-
67 resistance to the presence of small sample sizes and ability to deal with missing or incomplete data,
68 have been developed recently to model flood sensitivity. These include Naïve Bayes models (Liu

et al. 2016; Pham et al. 2020b; Tang et al. 2020) and regression tree models such as Random Forest (RF) models (Arabameri et al. 2020; Chen et al. 2020; Vafakhah et al. 2020), Decision Tree models (Khosravi et al. 2018; Costache 2019; Janizadeh et al. 2019; Pham et al. 2020a), Logistic Regression models (Shafapour Tehrany et al. 2017; Al-Juaidi et al. 2018; Tehrany and Kumar 2018). These regression tree models have become popular in the research environment due to their capability to model nonlinear phenomena such as floods.

Machine learning algorithms by default usually present point estimates only, and so decisions are made ignoring the uncertainty surrounding these estimates. In recent years, the use of ensemble models has attracted the attention of researchers in various fields as ensemble models benefit from several individual models and therefore tend to have better performance than individual models (Al-Abadi 2018; Tehrany et al. 2019a; Costache and Bui 2020; Shahabi et al. 2020). Bayesian Additive Regression Tree is one of the new ensemble models that combines Bayesian and Regression tree algorithms giving the access to the full posterior distribution of all unknown parameters in the model. This can be useful to reduce the uncertainty.

BART model has been used for modeling and predicting in different areas such as ecological processes (Plant et al. 2021) and gully erosion (Chowdhuri et al. 2020). Due to the fact that the flood is a non-linear phenomenon and has a lot of the uncertainty, use of appropriate models that have the ability to predict this phenomenon and reduce uncertainty is essential in the management, planning and prevention of flood risk. In the field of flood hazard modeling so far, very little attention has been paid to the role of hybrid Bayesian and Decision Tree algorithms. Therefore, the purpose of this study is to develop and present a new flood susceptibility model based on the ensemble type Bayesian Additive Regression Tree (BART) method. The new method will be

91 compared with the Naïve Bayes (Bayesian type) and Random Forest (regression tree type) based
92 models to evaluate the predictive performance of the new method.

93

94 **1.2. Study area**

95 The Kan River watershed is 200 km^2 and is located northwest of Tehran, Iran. This watershed is
96 located between latitudes 51° 10′ and 51° 23′ east and 35° 46′ and 35° 58′ north (Fig. 1). The
97 average height of the watershed is 2428 meters, the average slope of the whole watershed is 43.4%
98 and the most important river in this mountainous region is the Kan river. The study area is located
99 in the southern margin of the central Alborz region in terms of geological status and has a
100 mountainous climate with the average annual rainfall of 414.13 mm. The average annual discharge
101 of the Kan River is 2.2 m^3/s and its annual water flow is about 70 million m^3/year. Seven important
102 flood events have been reported in the Kan watershed since …, which have caused damage to
103 commercial and residential facilities, agricultural land and even caused casualties in the region
104 (Delkash et al. 2014).

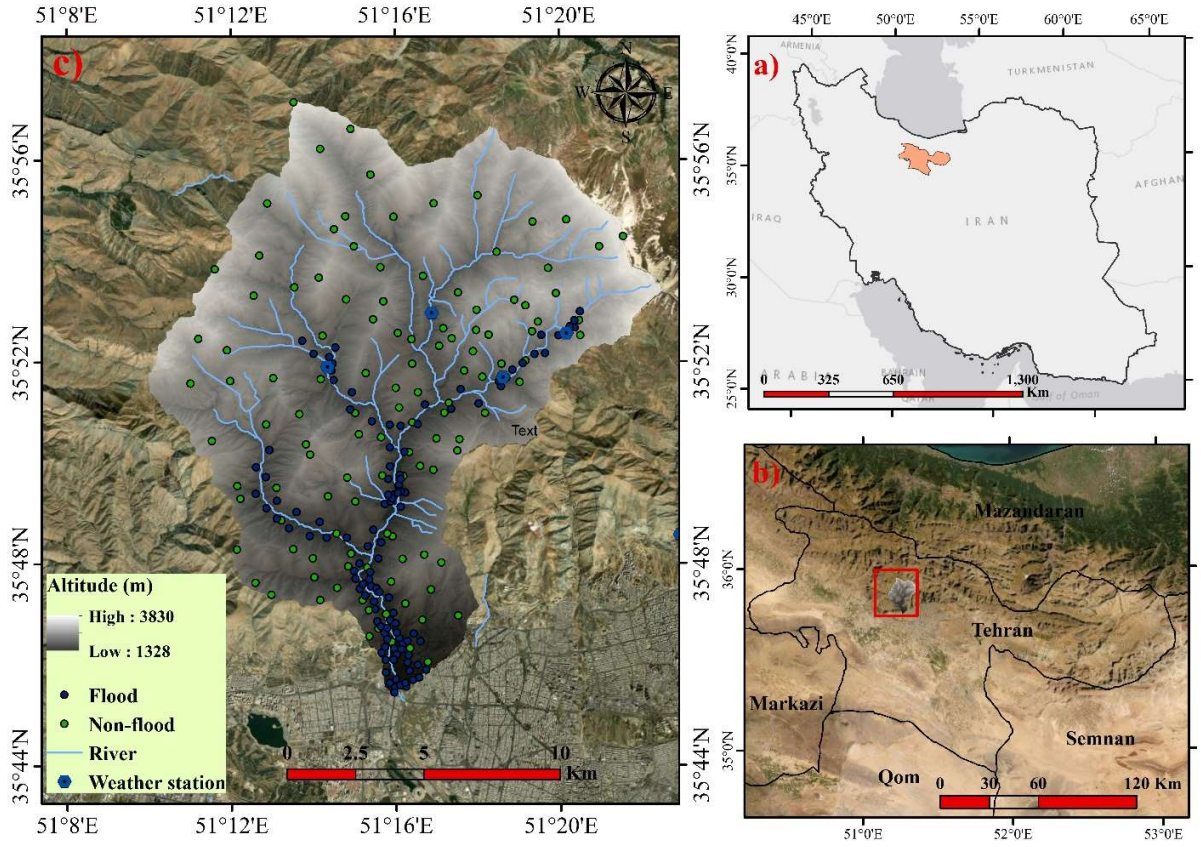

105

106 **Fig. 1. Location of case study a) country of Iran b) Tehran Province and c) Kan watershed**

107 ## 2. Material and methods

108 ### 2.1. Flood Inventory Data Preparation

109 In order to prepare a flood susceptibility map it is necessary to analyze the historical floods. The
110 Kan watershed has been severely affected by dangerous floods in recent decades, causing
111 extensive damage and casualties. According to historical floods recorded by the Regional Water
112 Company of Tehran Providence (1954/8/27, 1955/6/9, 1978/3/7, 1981/7/25, 1986/2/2, 1995/4/23,
113 1996/4/3), field visits and interviews with locals on 2019/10/5 to 2019/10/9 and the identification
114 of flood-affected areas by GPS equipment (Fig. 2), 118 flooding locations are identified in the
115 area. In addition to this, further 118 non-flood points were randomly placed in the inter-fluvial

area, or within very steep altitude where the flood phenomenon is almost impossible in the case study area. The position of all 236 locations are presented in Fig. 1. The data were divided into two categories of training and validation for modeling, so that 70% of the data were used for training and 30% for validation (Ahmadlou et al. 2019; Choubin et al. 2019). The flowchart of research methodology is given in Fig. 3.

Fig. 2. Example of a flood location in the Kan watershed

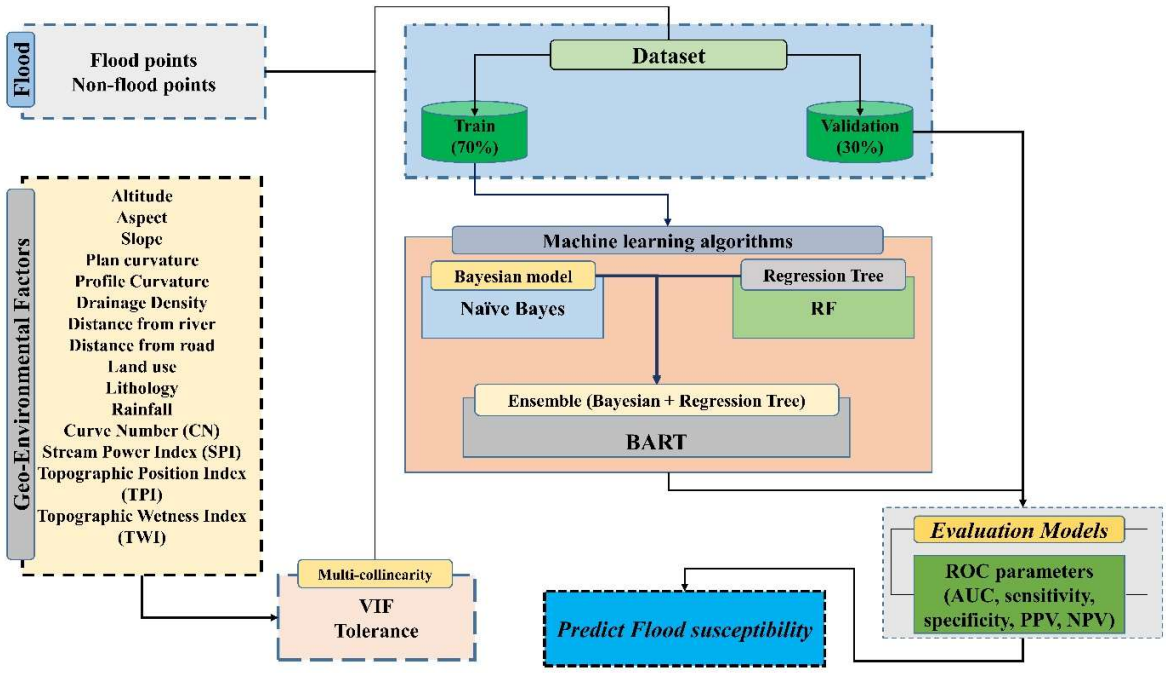

Fig. 3. Research Methodology

2.2. Spatial Data Preparation

Floods are one of the natural phenomena and are affected by various climatic and geo-environmental factors. In this study, the following 15 climatic and geo-environmental variables are used as potential explanatory factors for flood susceptibility at a given location: altitude, aspect, slope, plan curvature, profile curvature, drainage density, distance form river distance from road, stream power index (SPI), topographic wetness index (TWI), topographic position index (TPI), curve number (CN), land use, lithology and annual rainfall (Ngo et al. 2018; El-Magd et al. 2021).

The above 15 factors (i.e. potential flood susceptibility model independent variables) were confirmed as significant by using the multi-collinearity analysis. The multi-collinearity analysis evaluates the intensity of multiple correlations between considered variables by calculating the

138 variance inflation factors (VIFs). The higher the value of the VIF the more likely it is that that
139 variable does not play a significant role in flood susceptibility prediction (Miles 2014). In this
140 study, the threshold of 5 was used for VIF to identify significant independent variables (Tehrany
141 et al. 2019a; Hosseini et al. 2020). VIFs were estimated using the USDM package in R software.
142 The analysis has shown that all fifteen variables shown here have VIF values below the above
143 threshold (see section 4.1) hence they have all been used a potential explanatory factors for
144 predicting the flooding susceptibility.

145 The values of above 15 variables were prepared based on previous studies (see Fig 4, 5 and 6). For
146 this purpose, the digital elevation model (DEM) of the study area with resolution of 12.5×12.5 m
147 was developed with elevation data obtained using the type L-band Synthetic Aperture Radar
148 (PALSAR) (https://vertex.daac.asf.alaska.edu/#). The aspect map was prepared based on DEM at
149 nine class in the ArcGIS 10.5 software (Choubin et al. 2019; Janizadeh et al. 2019). The ground
150 slope is one of the important factors in the occurrence of floods in watersheds (Tehrany et al. 2015;
151 Chapi et al. 2017). The slope map was prepared based on the DEM in ArcGIS 10.5 software
152 (Khosravi et al. 2018).

153 The plan and profile curvature are the spatial parameters used in the preparation of flood maps of
154 watersheds. These variables were prepared in ArcGIS 10.5 software using a DEM (Rahmati et al.
155 2016; Hong et al. 2018). Drainage density of the study area in ArcGIS 10.5 environment was based
156 on line density extension (Mahmoud and Gan 2018; Zhao et al. 2019). Distance from rivers is one
157 of the most important factors affecting flooding of lands along the rivers (Tehrany et al. 2014;
158 Khosravi et al. 2016, 2018). This map was prepared using the Euclidean order in ArcGIS 10.5
159 software (Khosravi et al. 2018). Distance from the road is also a factor affecting flooding. This

160 variable was prepared using the 1:50,000 road map of Tehran province, the ArcGIS10.5 software
161 and the Euclidean extension, to determine distance from the road (Shafapour Tehrany et al. 2017).

162 The stream power index (SPI) is one of the important parameters for flooding in watersheds and
163 the following relationship is defined here (Tehrany et al. 2014; Shafizadeh-Moghadam et al. 2018):

164 $$SPI = Catchment\ Area * \tan(slope) \quad (1)$$

165 System for Automated Geoscientific Analyses Geographic Information System (SAGA GIS 2.6)
166 software was used to prepare this variable (Tehrany et al. 2014).

167 Topographic position index (TPI) indicates the topographic status of the area, with positive values
168 indicating high altitudes and negative values indicating low altitudes such as valleys (Papaioannou
169 et al. 2015). Due to the role of topographic shape in the formation of floods, this index is considered
170 as one of factors affecting floods and this variable was prepared using the SAGAGIS 2.6 software.
171 TWI measures the effect of local topography on runoff production and shows the long-term
172 moisture content of a landscape (Hong et al. 2018; Khosravi et al. 2019), hence this indicator is
173 one of the influential variables in flood risk assessment in watersheds. This variable was obtained
174 based on the following (Khosravi et al. 2019) in SAGAGIS 2.6 software:

175 $$TWI = \ln(Catchment\ Area/\tan(slope)) \quad (2)$$

176 Lithology is one of the important factors in watershed flooding due to its direct effect on the level
177 of permeability and surface runoff (Rahmati et al. 2016). The geological map of the Kan watershed
178 was prepared based on the 1:100,000 geological map of the Iranian National Cartographic Center
179 (NCC) and then turned into a raster layer with a resolution of 12.5 m. The lithology map of the
180 study area was divided into seven different classes. The soil type map was also prepared using the
181 data from the Administration of Natural Resources of Tehran Province and the vector file of this

map was created with a raster format with pixel size of 12.5 meters using the ArcGIS 10.5 software (Tehrany et al. 2014).

Land use is the result of the interrelationships of socio-cultural parameters and the potential of the land (Rahmati et al. 2016; Bui et al. 2018). Changes in land use and land cover can have significant impact on flooding in watersheds (Khosravi et al. 2018). This map was prepared using images of Landsat 8 satellite imagery OLI sensors in 2019 and using the maximum likelihood algorithm and supervised classification in the ENVI 5.1 software and divided into four classes: orchard, rangeland, residential and rocky lands.

In order to prepare the annual rainfall map, the rainfall data of 7 gauge stations (inside and outside the watershed) were used in the period 1994-2019. After carefully examining the various interpolation methods in the ArcGIS 10.5 software, the distribution of annual rainfall in Kan watershed was prepared based on the ordinary Kriging method.

One of the most important factors in the occurrence of floods is soil condition and different land uses, which directly affects the amount of water infiltration into the land. In other words, the curve number (CN) at the level of each area indicates the hydrological behavior of that area and its discharge regime during rainfall. In order to determine the CN map the land use map and the hydrological soil groups map were combined in the ArcGIS software environment. Then, based on the tables related to the CN for different land uses of watersheds and according to hydrological soil groups map, the value of CN was determined in the case of previous average humidity (Mahmoud and Gan 2018; Tang et al. 2018).

The data summary information of all independent variables is shown in Table 1.

Table 1. Information of independent variables

Variables	Data Type	Data Source	Data resolution
Elevation	Raster Grid	ALOS PALSAR DEM, (Alaska Satellite Facility)	12.5 m* 12.5 m resolution
Aspect			
Slope			
Plan Curvature			
Profile Curvature			
Drainage Density			
SPI			
TWI			
TPI			
Distance from River	Line and polygon coverage	Administration of Natural Resources, Department Tehran Province.	1:50000
Distance from Road	Line and polygon coverage		1:50000
LULC	Spatial/Raster grid	Landsat 8 OLI (USGS)	30 m spatial resolution
Lithology	Line, point and polygon coverage	Geological Map by country's mapping organization (Iran)	1: 100000
Rainfall	Station specific information	25 Years information of rain gage stations	Interpolation with same spatial resolution with other parameters
CN	Raster Grid	LULC and hydrological soil groups map	

204

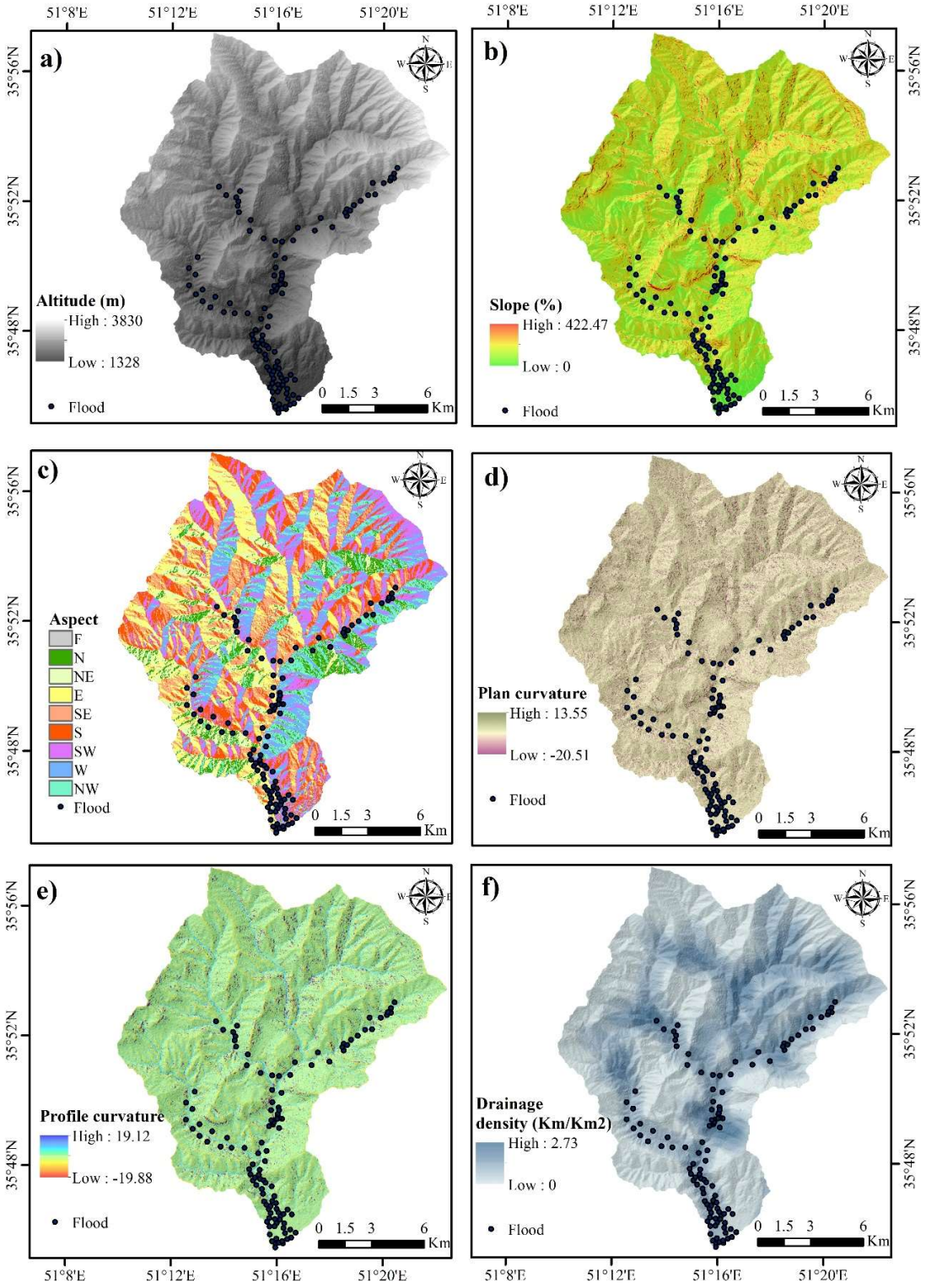

205

206 **Fig 4. Flood conditioning factors: a) altitude, b) aspect, c) slope, d) plan curvature, e) profile curvature, f)**
207 **drainage density**

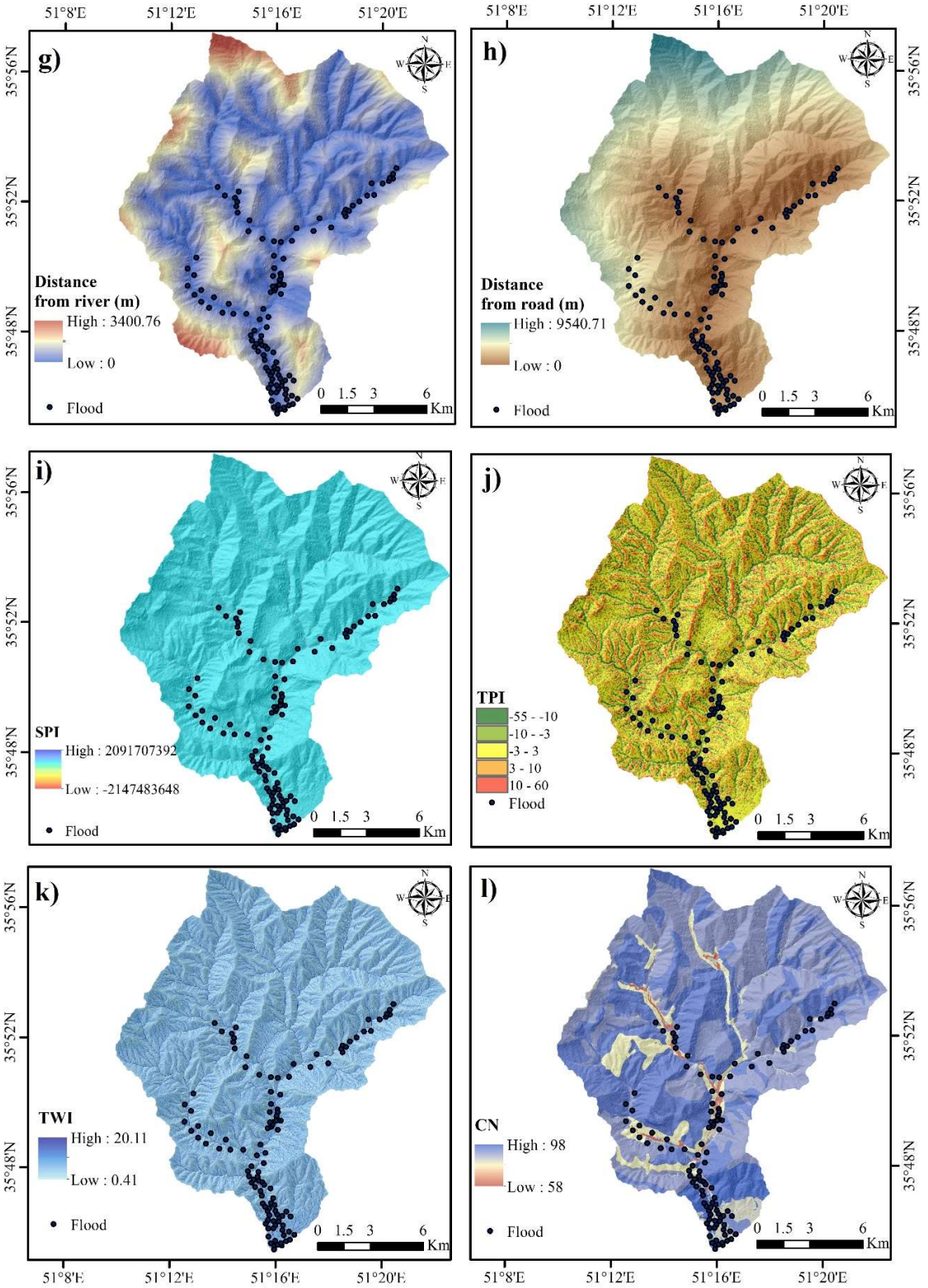

Fig 5. Flood conditioning factors: g) distance from river, h) distance from road, i) SPI, j) TWI, k) TPI, l) CN

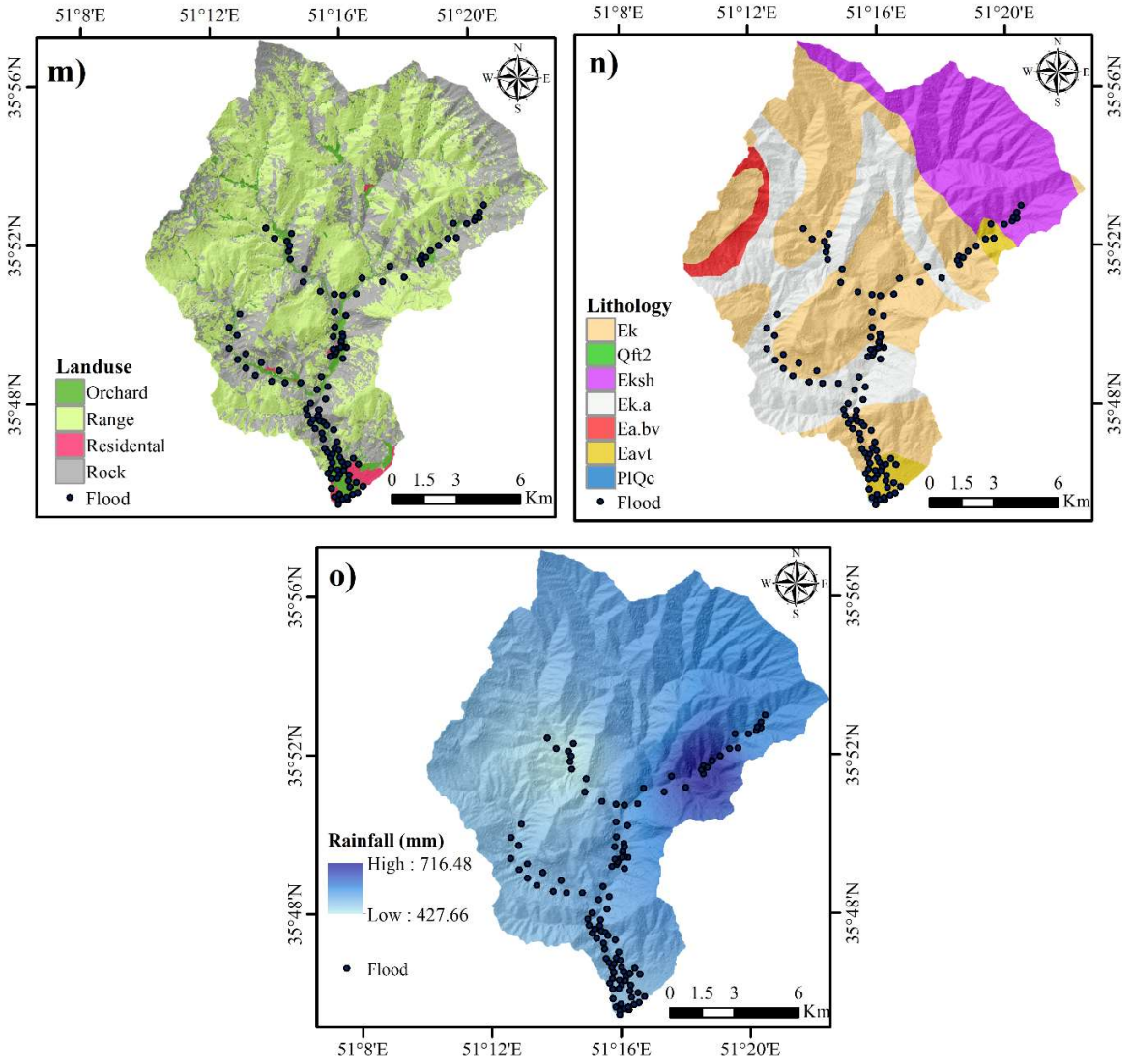

Fig. 6. Flood conditioning factors: m) land use, n) lithology and o) annual rainfall

2.3. Flood susceptibility models

This section describes three different models for predicting flood susceptibility: BART, NB and RF. All models are based on different machine learning methods that predict the flood susceptibility defined as the probability of flood occurrence at a given location of the analyzed

218 watershed. All three models have the same set of input variables, the fifteen explanatory /
219 independent variables described in section 2.3. These model inputs were determined in all cases
220 using correlation and multi-collinearity analysis (see next section). Finally, all models are trained
221 and tested using the data described in the next section.

222

223 **2.3.1. Naïve Bayes Model**

224 The Bayesian method is a way of classifying phenomenon based on the probability of that
225 phenomenon occurring or not occurring. Based on the inherent characteristics of probability
226 (especially probability division), Naive Bayes method offers good results after receiving the initial
227 practice (Rish and others 2001). Learning method in the simplest way, the base is the type of
228 learning with the supervisor. Bayes suggests a way to calculate the posterior probability, P (c | x),
229 from P (c), P (x) and P (x | c). The Naive Bayes classifier assumes that the effect of the predictor
230 cost (x) on a given category (c) of the different predictor values is neutral. This assumption is
231 known as conditional independence:

232 $$P(c|x) = \frac{P(C|X)*P(c)}{P(x)} \quad (3)$$

233 $$P(c|X) = P(x_1|c) * P(x_2|c) * \ldots * P(x_n|c) \quad (4)$$

234 where $P(c|x)$ is posterior probability of target, $P(c)$ is prior probability of class and $P(x)$ is the
235 prior probability of predictor (Zhang 2004). The e1071 package in R software was used for Naïve
236 Bayes modeling.

237 **2.3.2. Random Forest Model**

Random Forest (RF) method is a relatively complex method in which several decision trees are trained in order to increase the predictive accuracy of the model. The result is a prediction of a group of decision trees. In the random forest learning method, each decision tree is taught using a random sample selected from the training data set. The total selection of predictive variables used to divide nodes is also random. In the random forest method, the two properties *mtry* and *ntree* are determined for the number of auxiliary variables used in each subset and the number of trees used in the forest, respectively. One of the advantages of a random forest is that it can be used for both classification and regression type models. Random forest has parameters similar to the decision tree or "Bagging Classifier". Random forest adds randomness to the model as trees grow. Instead of searching for the most important features when dividing a "node", this algorithm looks for the best features among a random set of features. This leads to more variety and ultimately a better model. Therefore, in a random forest, only one subset of features is considered by the algorithm to divide a node. By adding a random threshold for each attribute, instead of searching for the best possible threshold, trees can be made even more random (Liaw et al. 2002). The randomForest package in R software was use for the RF modeling here.

2.3.3. Bayesian Additive Regression Tree (BART) Model

BART is a Bayesian approach to non-parametric output estimation using regression trees. The regression trees are relying on the return of the binary division of the predictive space into a set of superconductors to approximate certain unknown functions. The predictive space has dimensions corresponding to the number of variables. Tree-based regression models are capable of generating plenty of interaction and nonlinearity (Hill et al. 2020). Models consisting of a number of regression trees are more capable of capturing interaction and nonlinearity than single trees, as are additives in f.

BART can be considered a general collection of trees with a new estimation method based on a complete Bayesian probability model. The BART model can be expressed as follows:

$$P(Y = 1|X) = \varphi(\tau_1^N(X) + \tau_2^N(X) + \cdots + \tau_n^N(X) \quad (5)$$

where φ denotes the cumulative density attribute of the prevalent regular distribution. In this formulation, the sum-of-trees model serves as an estimate of the conditional probit at x which can be besides issues modified into a conditional threat estimate of Y = 1 (Kapelner and Bleich 2013). The bartMachine package in R software was use for BART modeling.

2.3.4. Model Validation and Performance Assessment

The ROC curve characterizes the relative performance of each model. The ROC curve is a graph in which the true positive (or specificity value) is shown in the vertical axis whilst the false positive (or sensitivity) is shown on the vertical axis (Frattini et al. 2010). For the sensitivity or a proportion of occurrence pixels that have been correctly predicted, the larger this value the more accurate the model is in determining the occurrence points. Also, the feature means a ratio of non-occurring pixels that the model correctly predicted. The area under the curve (AUC) measures one aspect of performance. The value of AUC varies from 0 to 1, where the value of 0.5 denotes the random prediction and 1 denotes the perfect prediction (Yesilnacar and Topal 2005). In this study, the following equations have been used to calculate true positive rate (TPR), true negative rate (TNR), specificity, sensitivity and AUC:

$$TPR = \frac{TP}{(TP+FN)} \quad (6)$$

$$TNR = \frac{TN}{(TN+FP)} \quad (7)$$

281 $$Sensitivity = \frac{Number\ of\ positives}{(Number\ of\ positives + Number\ of\ false\ positives)} \quad (8)$$

282 $$Specificity = \frac{Number\ of\ true\ negatives}{(Number\ of\ true\ negatives + Nu \quad of\ false\ negatives)} \quad (9)$$

283 $$AUC = \frac{\sum TP + \sum TN}{(P+N)} \quad (10)$$

284 where, TP (true positive) and TN (true negative) are truly classified pixel numbers, while FP (false
285 positive) and FN (false negative) are falsely classified pixel numbers; P is the total number of
286 floods and N is the total number of non-floods (Choubin et al. 2019; Khosravi et al. 2019).

287

288 **3. Results**

289 **3.1. Analysis of Independent Variables**

290 In order to build a flood susceptibility model, potential model input variables are first analyzed for
291 independence (via correlation) and linearity (via multi-collinearity analysis).

292 The results of the correlation study of the variables used in flood susceptibility modelling based
293 on Spearman correlation test are shown in Fig.7. As it can be seen from this figure, the analyzed
294 variables have a relatively low correlation with each other hence these were all selected for further
295 analysis.

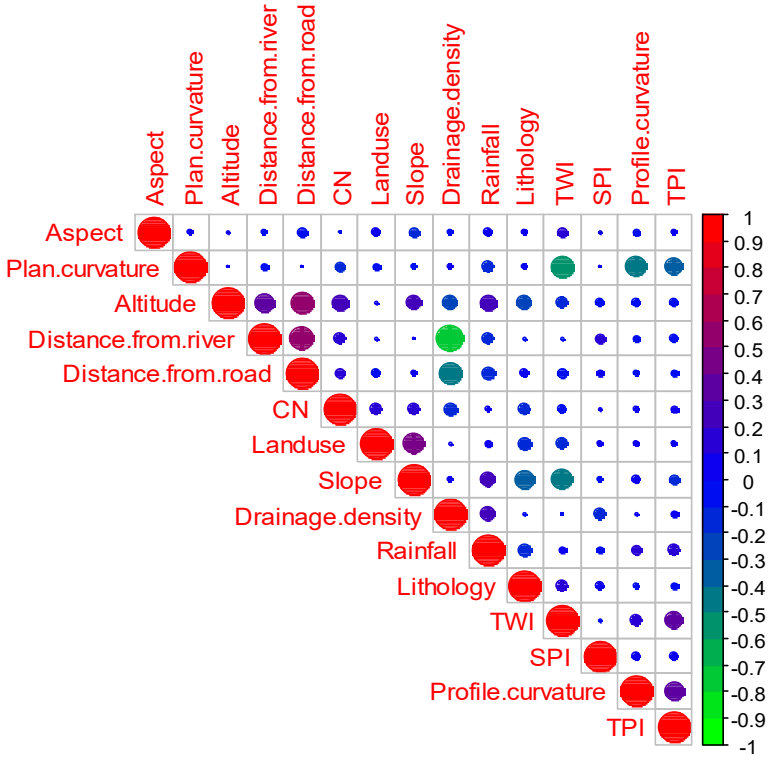

296

297 **Fig. 7. Correlation analyses between independent variables**

298

299 In order to determine the appropriate inputs for flood susceptibility modelling, multiple
300 multiplexing and tolerance tests were used using *usdm* package (in the R software environment).
301 In order to investigate the linearity of the VIF range, all variables with VIF value smaller than 5
302 were considered.

303 The results of multi-colinearity and tolerance analyses are shown in Table 2. The study of the
304 linearity of the variables shows that all analyzed variables have a VIF value smaller than 5. The
305 highest linearity was obtained for distance from the river with VIF equal to 2.39 and the tolerance
306 equal to 0.42. The smallest linearity was obtained for the aspect variable with VIF of 1.07 and

307 tolerance of 0.93. Based on this, all variables shown in Table 2 are selected as potential inputs into
308 the flood susceptibility model.

309 **Table 2. Multi-collinearity analysis base on VIF and Tolerance to determine the linearity of the independent**
310 **variables**

Variables	VIF	Tolerance
Altitude	2.09	0.48
Aspect	1.07	0.93
Slope	1.57	0.64
Plan curvature	1.9	0.53
Profile Curvature	1.47	0.68
Drainage density	2.33	0.43
Distance from River	2.39	0.42
Distance from road	2.09	0.48
SPI	1.09	0.92
TPI	1.37	0.73
TWI	2.01	0.50
CN	1.35	0.74
Land use	1.29	0.77
Lithology	1.27	0.79
Rainfall	1.46	0.68

311

312 ## 3.2. Tuned parameters

313 The tuned parameter values for the BART model are shown in Table 3 and Figure 8.

314 Table 3. Tune parameters in BART model

Parameters	Tuned value
Number of trees	100
Number burn in	500
Number iteration after burn in	1000
Alpha	0.95
Beta	2
K	2
Q	0.9

315

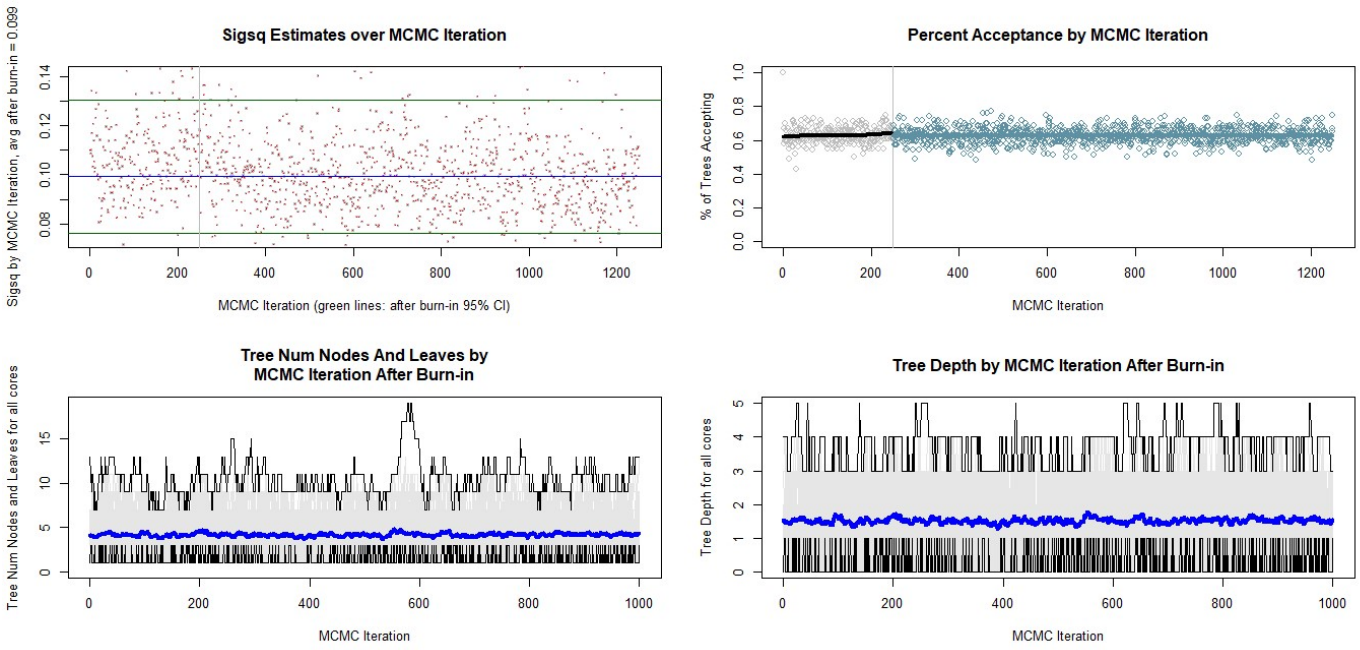

316

317 **Fig. 8. The result of the BART model for flood susceptibility**

318 ## 3.3 Model Validation

319 ROC curves parameters include sensitivity, specificity, NPV, PPV and area under curve (AUC).
320 These parameters were used to evaluate the efficiency of Naïve Bayes, RF and BART models. The
321 corresponding results for the training and testing stages of these models are shown in Figs. 9 and
322 10 and Table 4.

323 According to the results obtained in the training phase, the sensitivity statistics in NB, RF and
324 BART models are equal to 0.76, 0.99 and 0.99, respectively. This shows the high sensitivity of the
325 three models and their accuracy. The specificity statistics for the NB, RF and BART models are
326 equal to 0.89, 0.95 and 0.90, respectively. The PPV statistics of 0.74, 0.95 and 0.91 and the NPV
327 statistics of 0.77, 0.99 and 0.98 were obtained for the NB, RF and BART models, respectively.
328 This shows the high accuracy of these models in predicting the non-occurrence points. The results
329 of model evaluation based on the AUC show that the accuracy of NB, RF and BART models is

330 0.88, 0.99 and 0.89, respectively. Therefore, all three models have high predictive accuracy at the
331 training stage.

332 Evaluation of the three models at the validation stage shows that the sensitivity statistics for NB,
333 RF and BART models are equal to 0.76, 0.91 and 0.94, respectively. This shows the high
334 sensitivity of these models in flood estimation. The specificity statistics in the NB, RF and BART
335 models are equal to 0.75, 0.72 and 0.78, respectively. Evaluation of the same three models based
336 on PPV and NPV statistics result in PPV values of 0.74, 0.75, 0.80, and NPV values of 0.77, 0.90,
337 and 0.93 respectively, indicating high accuracy of these models when predicting non-flood points
338 compared to flood points. For the overall evaluation of the models at the validation stage, the AUC
339 statistic was used too and the values obtained for the NB, RF and BART models are equal to 0.81,
340 0.85 and 0.89, respectively.

341 **Table 4. The results of evaluating the efficiency of Naïve Bayes, RF and BART models in train and validation**
342 **stage**

Models	Stage	Parameters				
		Sensitivity	Specificity	PPV	NPV	AUC
Naïve Bayes	Train	0.76	0.89	0.87	0.78	0.88
	Validation	0.76	0.75	0.74	0.77	0.81
RF	Train	0.99	0.95	0.95	0.99	0.99
	Validation	0.91	0.72	0.75	0.90	0.85
BART	Train	0.99	0.90	0.91	0.98	0.98
	Validation	0.94	0.78	0.80	0.93	0.89

343

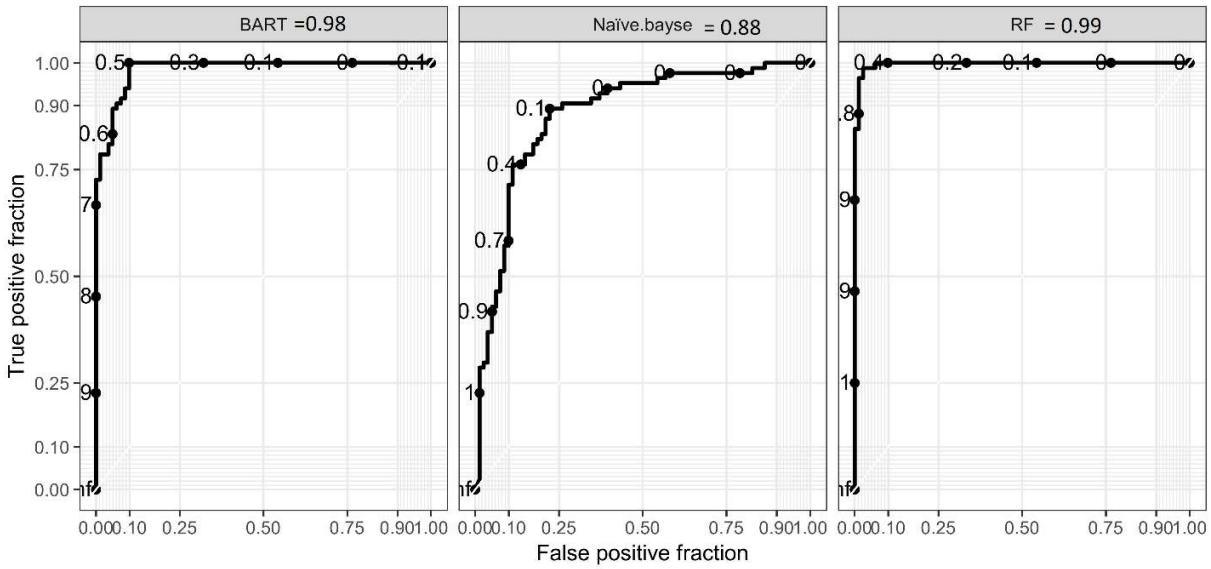

344

345 **Fig. 9. The ROC curve analysis for Naïve Bayes, RF and BART models using the train dataset**

346

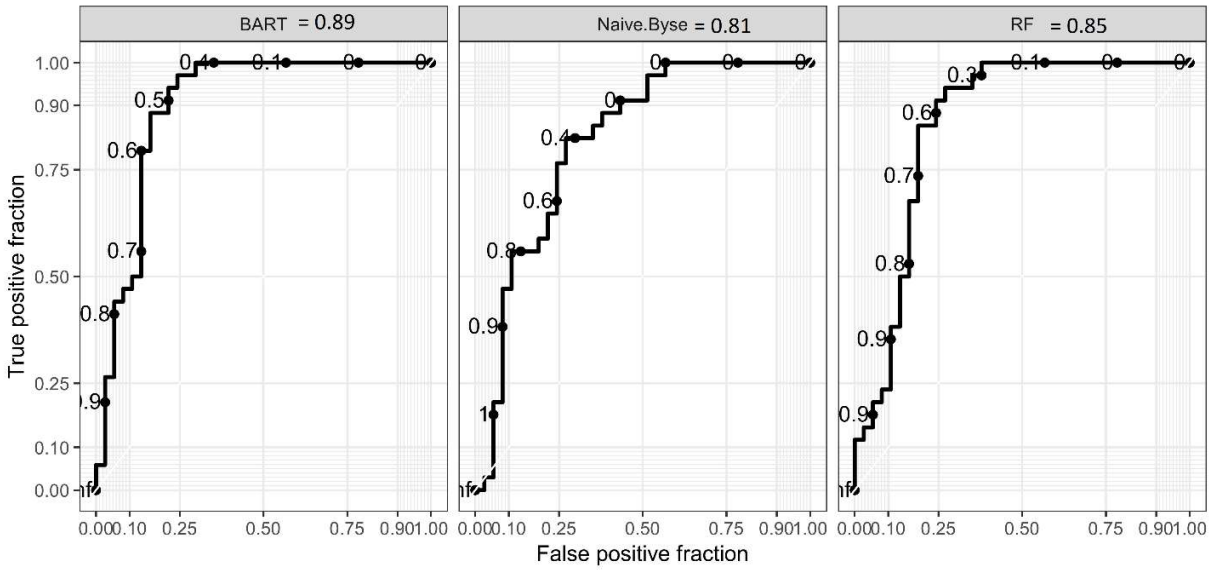

347

348 **Fig. 10. The ROC curve analysis for Naïve Bayes, RF and BART models using the testing dataset.**

349

350

351

352

353 **3.4. Flood susceptibility modeling results**

354 After modelling the flood sensitivity using NB, RF and BART models and evaluating the
355 efficiency of these models, flood susceptibility was forecasted for the whole analyzed watershed.
356 The final map was divided into five flooding susceptibility classes (very low, low, moderate, high
357 and very high) by using the natural break algorithm (Fig. 11). According to the map obtained,
358 flooding susceptibility is the highest sensitivity around the main river and the areas near the outlet
359 of the watershed, which have a lower altitude. At the same time, most of the area analyzed, which
360 is generally high altitude, has a very low sensitivity.

361 The results of the area and percentage covered by each susceptibility class are shown in Table 5.
362 According to the results, the area of very high susceptibility class is equal to 22.11 km^2 (10.26%)
363 in the NB model, 21.23 km^2 (9.85%) in the RF model and 19.48 km^2 (9.04%) in the BART model.
364 However, the BART model, with 50.5 km^2 (23.5%) has predicted the largest area with very high
365 and high susceptibility classes.

366 In order to evaluate the validity of the predicted flood susceptibility maps in relation to the
367 identified flood points in the study area, the frequency ratio (FR) approach was used (Fig. 9). As
368 it can be seen from Figure 12, the highest frequency ratio is in very high and high classes, which
369 indicates the appropriate prediction of the models used for flood-susceptibility areas. However,
370 the predictions of the RF and BART models that are in the very high class are much higher than
371 the corresponding class predictions made by two other models, which indicates a more accurate
372 prediction of flood susceptibility in this area.

373

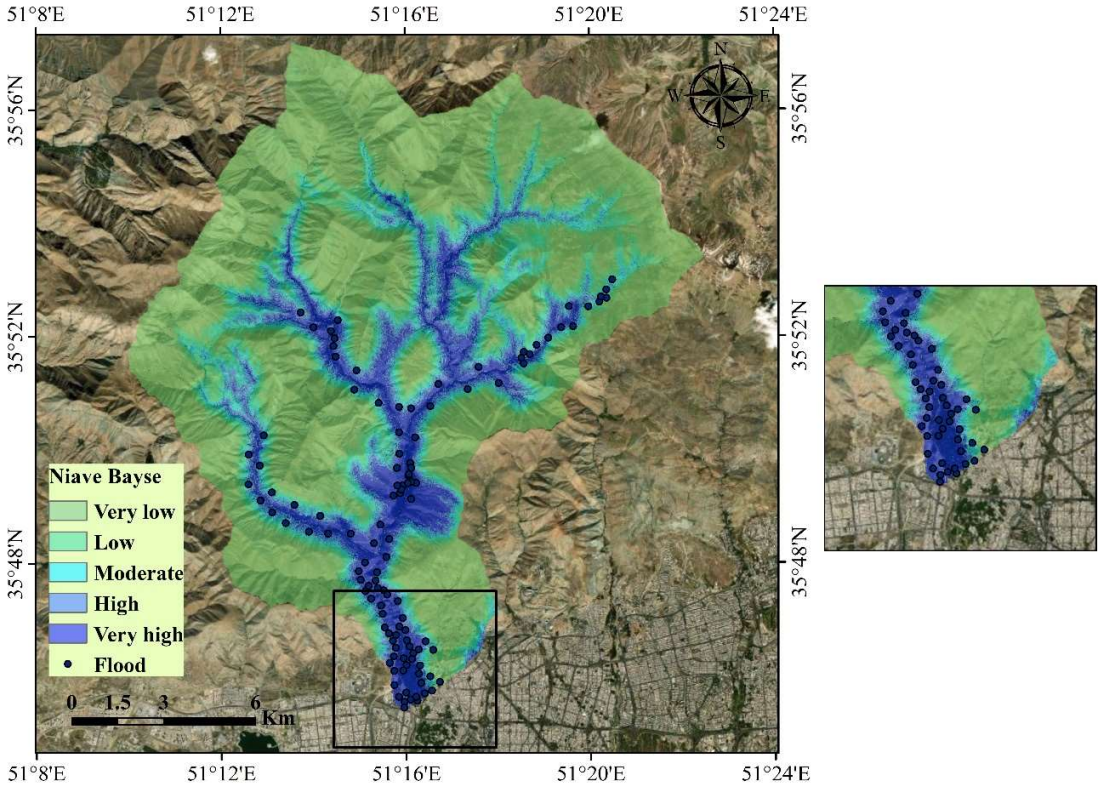
51°8'E
51°12'E
51°16'E
51°20'E
51°24'E
35°56'N
35°52'N
35°48'N
N
W
E
S
Niave Bayse
Very low
Low
Moderate
High
Very high
Flood
0 1.5 3 6
Km

374

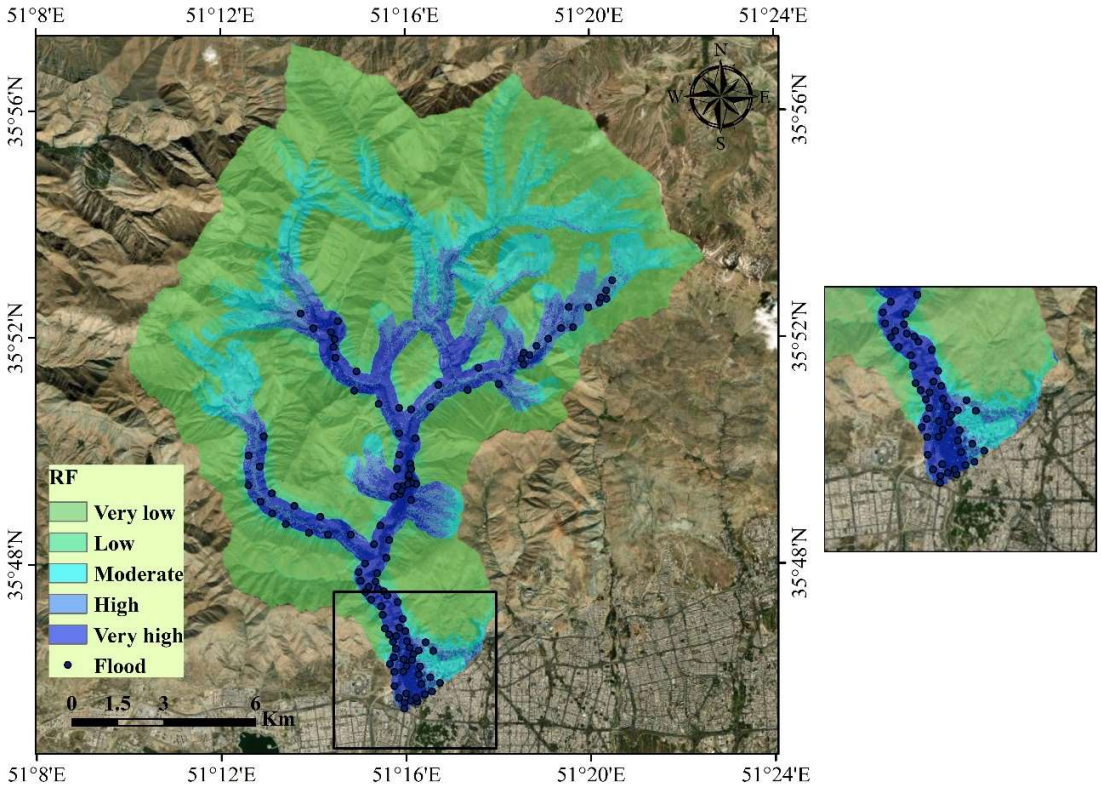
51°8'E
51°12'E
51°16'E
51°20'E
51°24'E
35°56'N
35°52'N
35°48'N
N
W
E
S
RF
Very low
Low
Moderate
High
Very high
Flood
0 1.5 3 6
Km

375

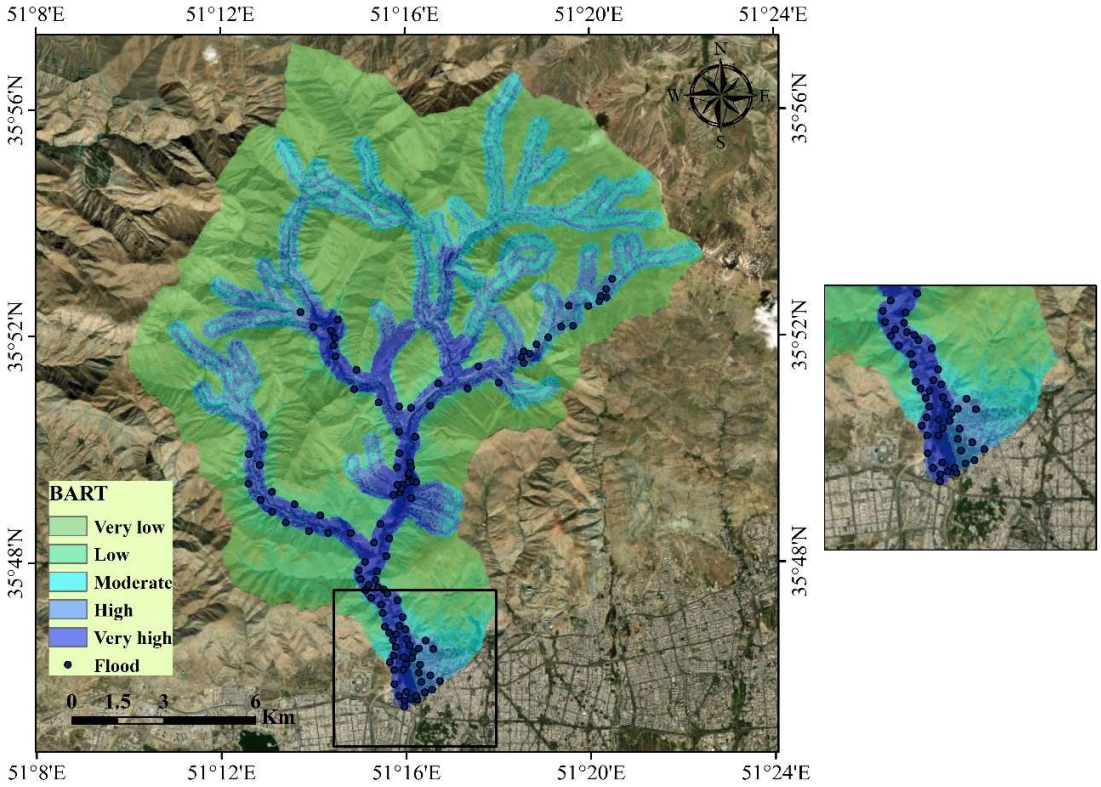

Fig. 11. Flood susceptibility map using the Naïve Bayes, RF and BART models

Table 5. The watershed area (in km^2 and %) in each flood susceptibility class

Susceptibility class	NB model		RF model		BART model	
	Area (km^2)	Area (%)	Area (km^2)	Area (%)	Area (km^2)	Area (%)
Very low	121.85	56.52	112.32	52.10	106	49.17
Low	31.53	14.62	33.24	15.42	28.39	13.17
Moderate	21.67	10.05	31.04	14.40	30.65	14.22
High	18.44	8.55	17.77	8.24	31.08	14.42
Very High	22.11	10.26	21.23	9.85	19.48	9.04

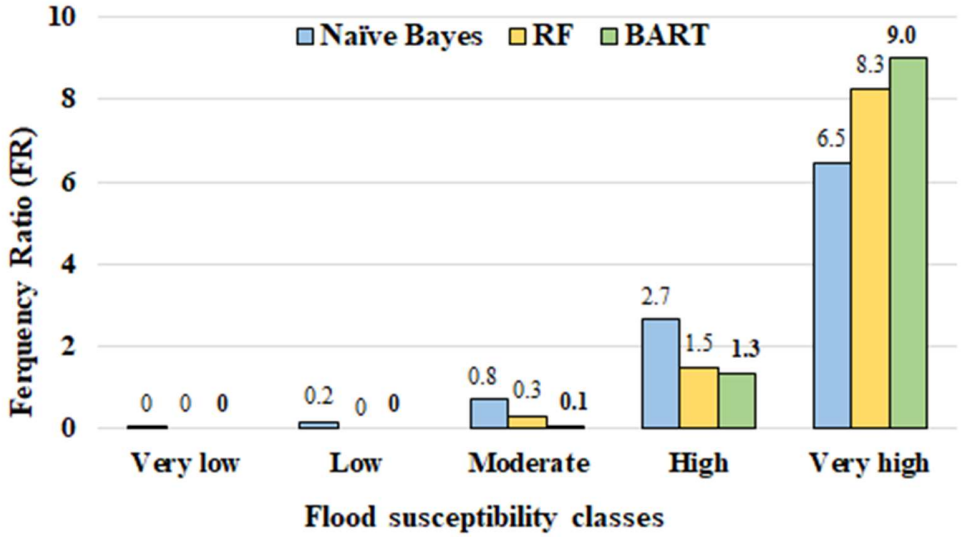

Fig. 12. Analysis of the frequency of floods on the flood susceptibility maps predicted using the FR method

3.5. Explanatory Variable Importance

The results of the importance of the independent (i.e. input) variables used to model the flood susceptibility using the three models are shown in Fig. 13. It is clear that in the three models used different input variables have different effects on determining the flood susceptibility. It is also clear that altitude and distance from the river are more important than other variables in all three models.

Due to the importance of 4 variables (altitude, distance from the river, distance from the road and rainfall) on flood susceptibility in the BART model, these 4 variables were further investigated (Fig. 14). As it ca be seen from Fig. 14, the flood susceptibility decreases with increasing altitude, with highest sensitivity to floods being at an altitude of 1400 meters (which is close to the altitude of the outlet of the watershed). This indicates the inverse relationship between the altitude and the flooding susceptibility. Further, a study of the distance from the river shows that locations with distances smaller than 500 meters have a high susceptibility to flooding whilst locations with

distances larger than 500 meters from the river have a decreasing flooding susceptibility which stabilizes around a low value for the distances of 1000-1500 meters. Regarding the distance from the road, it can be noted from Fig 14 that the flooding susceptibility decreases with the increasing distance from the road with most sensitive areas being located less than 1000 meters from the road. Finally, a study of the effect of rainfall on flooding susceptibility shows that areas with 450 to 500 mm of rainfall per year are more sensitive than the areas with higher rainfall (the susceptibility decreases so that from rainfall 550 to 650 mm it is low and constant).

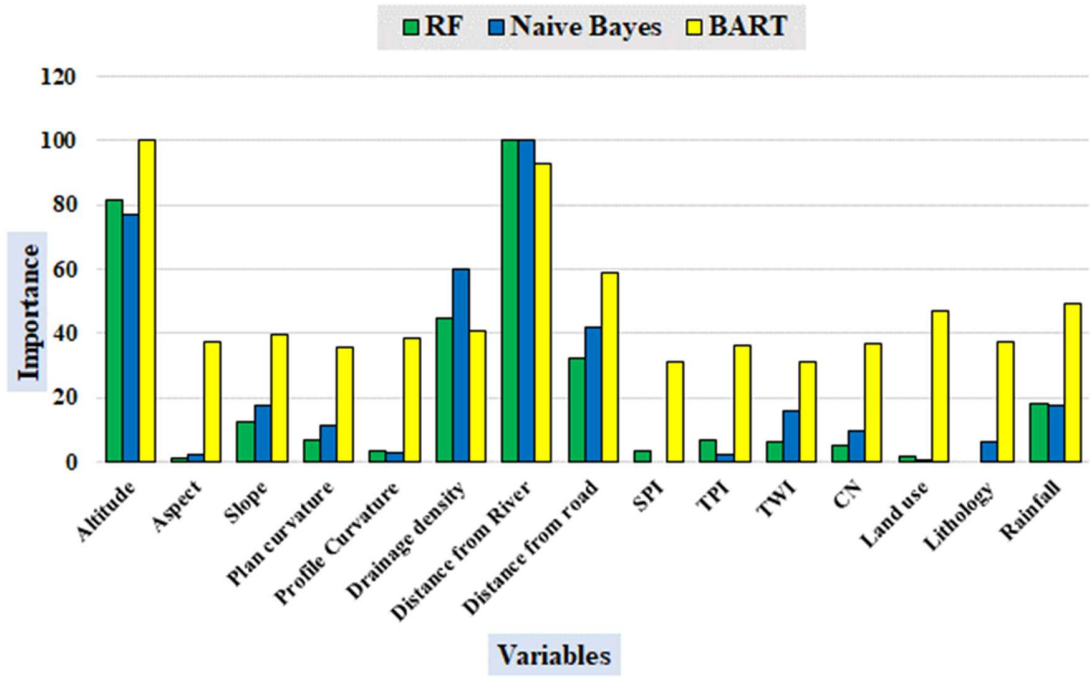

Fig. 13. Results of relative importance of independent variables in flood sensitivity modeling in Naïve Bayes, RF and BART models

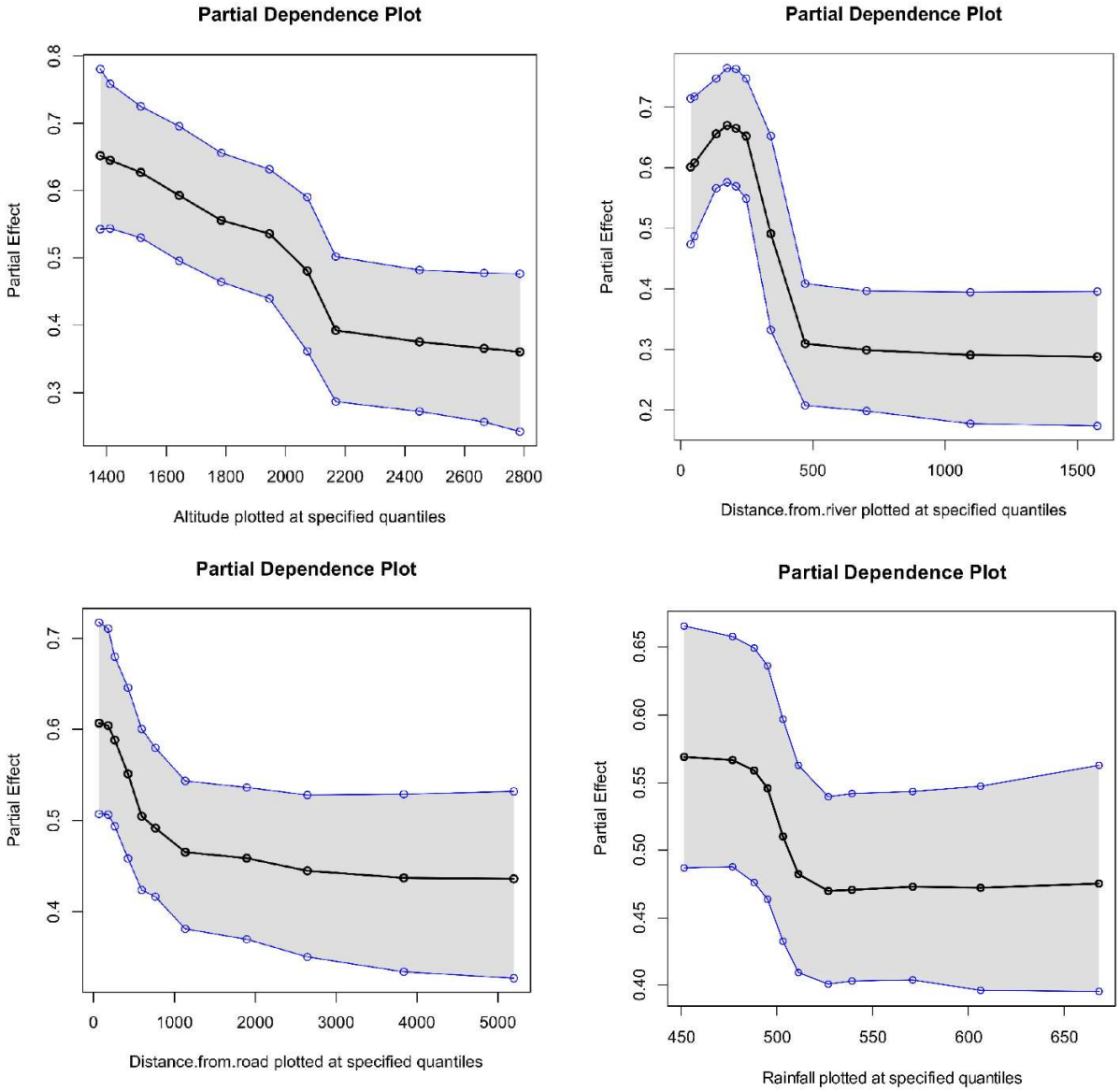

408

409 **Fig 14. Partial effect plot for four importance variable (altitude, distance from river, distance from road and**

410 **rainfall)**

411

412 ## 4. Discussion

413 In the present study, we developed and presented a novel flood susceptibility BART model that is

414 based on machine learning and Bayesian approach. In addition, two existing models, NB and RF

were used for comparison. The results obtained showed that all three models have a high performance in predicting the flooding susceptibility in the Kan watershed in Iran but, based on the model performance criteria, the new BART model has outperformed the other two models. In terms of input variable importance, the results obtained show that the altitude and distance from the river are the most important variables for assessing flooding susceptibility in the study area.

One of the main objectives of this study was to apply the BART model and evaluate the efficiency of this model in flood modeling in the study area. Performance evaluation of NB, RF, and BART models shows that the BART model performed best in the validation stage in terms of predicting flood susceptibility. The use of the Bart model in Natural Hazard studies and especially flood sensitivity modeling has been reported rarely before. The efficiency of this model has been proven in other fields such as forest science. Ahmadi et al. (2021) used BART model to mapping forest stand characteristics and showed that this model has a high performance in comparison to other models.

The BART model is a non-parametric Bayesian regression approach that uses consistent basic random elements. Bayesian Additive Regression Trees (BART) provides a flexible way to fit a variety of regression models while avoiding strong parametric assumptions (Hill et al. 2020). The tree ensemble model is supported by an uncertainty framework in the Bayesian inferential framework and provides a principled approach to regulation through previous specifications (Pratola and Higdon 2016; Sparapani et al. 2016). This model uses a non-parametric tree aggregation model to allow flexibility of the average structure of a regression. But it also has the advantages of a Bayesian inferential framework given the amount of uncertainty and its regulation through calibrated data locations (Sparapani et al. 2016; Hill et al. 2020; Prado et al. 2021; Wu et al. 2021).

438 One of the main advantages of the BART model is the capacity to form inference on numerous
439 features of the survival distribution directly from the posterior samples. As a Bayesian model,
440 BART consists of a set of priors for the construction and the leaf parameters and a possibility for
441 data in the terminal nodes (Pratola and Higdon 2016; Sparapani et al. 2016). The object of the
442 priors is to afford regularization, limiting any single regression tree from dominating the total fit.
443 Many Machine learning (ML) models suffer from missing data problems. BART model has a
444 specialty that provides the user with the straight designation missing covariate data within the
445 BART structure. This method combines missing data indicators into the training data set and
446 supports for divisions on the missing indicators, guiding to raised efficiency under a pattern
447 ensemble model structure (Hill et al. 2020; Prado et al. 2021; Sparapani et al. 2021).

448 Determining the importance of independent variables in flood susceptibility modeling in the Kan
449 watershed showed that altitude, distance from river, distance from road and rainfall variables are
450 important factors affecting flood susceptibility in this region. A study of altitude variable shows
451 that low altitudes, which are often at the outlet of watersheds, are highly susceptible to flooding,
452 which is consistent with the findings of Khosravi et al. (2019), Pham et al., (2020a).

453 Distance from river is another important factor in flood susceptibility in the Kan watershed, and
454 the results indicate the sensitivity of areas close to the river. Ahmadlou et al., (2019) showed in
455 their studies that areas 500-1000 meters from the river are highly sensitive to flooding. Given that
456 the flood-prone areas are located near the river and the reason is due to rise of flow from the river
457 channels (Choubin et al. 2019; Darabi et al. 2019; Panahi et al. 2021), in the Kan watershed, due
458 to lack of observance of riverbed and river boundaries, several restaurants and villas have been
459 built in the areas near the river, and due to the presence of more orchard in the river area, has led
460 to the obstruction of flow in these areas and has increased the sudden release of flood current.

461 Invasion of the river boundaries and the create of orchard in it, in addition to causing financial
462 damage to the residents of the area, also by blocking the flow in sections such as tunnels, will
463 cause secondary floods and intensify the damage to the people and downstream areas.

464 Another factor affecting the flood susceptibility in the Kan watershed is the distance from road.
465 Construction and crate of communication roads will increase the runoff and runoff speed because
466 it will reduce the area of the existing surface to absorb rainfall and thus will increase the sensitivity
467 to flooding in these areas (Tehrany et al. 2019b; Zhao et al. 2019).

468 The study of the rainfall indicates that areas with less rainfall are highly susceptible to flood, which
469 are mainly areas close to the outlet of the Kan watershed. Due to the mountainous nature of the
470 region, most of the precipitation in the upstream areas of the Kan watershed is snow, so in these
471 areas the possibility of infiltration is higher. In addition, precipitation in the downstream areas is
472 in the form of storms and these storms are usually more severe in the autumn and causes the river
473 inundation and flooding.

474 In recent years, due to human interventions and the resulting climate and land-use changes, the
475 rate of flooding and the corresponding damages have increased significantly. Studies such as this
476 one allow managers to reduce flood risks through planning and flood susceptibility analysis.
477 Therefore, we are always looking for more accurate modeling approaches to reduce the bias in the
478 prediction of flood susceptibility. In the present study, we showed that BART model is an accurate
479 model that can be used for effective flood susceptibility modeling. This model can be applied in
480 the future along with other modes that have shown high ability in flood modeling studies.

481

482 **5. Conclusion**

Floods are one of the most frequent and destructive natural disasters that can cause a lot of damage. In order to investigate and analyze the susceptibility of some are to flooding, different methods have been developed by the researchers.

In this study, the Bayesian based model (Naïve Bayes), regression tree type model (Random Forest) and ensemble type model (Bayesian Additive Regression Tree - BART) were developed to predict flood susceptibility in the Kan watershed. A total of 15 explanatory (i.e. model input) variables were used after multi-collinearity analyses as independent variables and 118 flood locations and 115 non-flood locations after field surveys and the use of available information as a dependent variable for flood modeling.

The validation results obtained for flood susceptibility modeling showed that the Naïve Bayes, RF and BART models all have a good predictive performance. However, the new BART model has the higher prediction accuracy than the Naïve Bayes and RF models. This is due to the fact that it uses features of both methods in the ensemble setting.

The analysis of the importance of explanatory variables showed that the effect of independent variables is different in each model. However, the altitude and distance from the river were more important than other variables in all three models meaning that low-height areas and areas close to the river are more susceptible to flooding.

The Kan watershed is close to the city of Tehran and the pleasant climate of this tourist area has caused that its riverbanks are occupied with many constructions that have been carried out. These areas receive a large number of tourists in spring and summer and hence are strongly affected by the floods. It is therefore necessary to provide flood hazard maps for the region. The results of this

research can be used as a baseline map in development projects to determine areas susceptible to flooding hence prevent the construction in these high-risk areas.

Author Contributions: Saeid Janizadeh acquired the data; Saeid Janizadeh and Mehdi Vafakhah conceptualized and performed the analysis; Saeid Janizadeh wrote the manuscript and discussion, and analyzed the data; Mehdi Vafakhah, Zoran Kapelan and Naghmeh Mobarghaee Dinan provided technical sights, as well as edited, restructured, and professionally optimized the manuscript. All authors discussed the results and edited the manuscript. All authors have read and agreed to the published version of the manuscript.

Ethical Approval: We confirm that this manuscript has not been published elsewhere and is not under consideration by another journal.

Consent to Participate: All authors have participated the manuscript and agree with submission to Water Resources Management.

Consent to Publish: All authors have approved the publication of this manuscript in the Water Resources Management Journal.

Availability of data and materials: We have no permission to release data and codes.

Funding: The authors received no specific funding for this work.

Acknowledgments: We acknowledge Tarbiat Modares University's support for this work.

Conflicts of Interest: The authors declare no conflict of interest.

References

Ahmadlou M, Karimi M, Alizadeh S, et al (2019) Flood susceptibility assessment using integration of adaptive network-based fuzzy inference system (ANFIS) and biogeography-based optimization

526 (BBO) and BAT algorithms (BA). Geocarto Int 34:1252–1272
527 Al-Abadi AM (2018) Mapping flood susceptibility in an arid region of southern Iraq using ensemble
528 machine learning classifiers: a comparative study. Arab J Geosci 11:218
529 Al-Juaidi AEM, Nassar AM, Al-Juaidi OEM (2018) Evaluation of flood susceptibility mapping using
530 logistic regression and GIS conditioning factors. Arab J Geosci 11:765
531 Arabameri A, Saha S, Chen W, et al (2020) Flash flood susceptibility modelling using functional tree and
532 hybrid ensemble techniques. J Hydrol 125007
533 Bui DT, Panahi M, Shahabi H, et al (2018) Novel hybrid evolutionary algorithms for spatial prediction of
534 floods. Sci Rep 8:15364
535 Chapi K, Singh VP, Shirzadi A, et al (2017) A novel hybrid artificial intelligence approach for flood
536 susceptibility assessment. Environ Model Softw 95:229–245
537 Chen W, Li Y, Xue W, et al (2020) Modeling flood susceptibility using data-driven approaches of
538 na{\"\i}ve bayes tree, alternating decision tree, and random forest methods. Sci Total Environ
539 701:134979
540 Choubin B, Moradi E, Golshan M, et al (2019) An ensemble prediction of flood susceptibility using
541 multivariate discriminant analysis, classification and regression trees, and support vector machines.
542 Sci Total Environ 651:2087–2096
543 Chowdhuri I, Pal SC, Arabameri A, et al (2020) Implementation of artificial intelligence based ensemble
544 models for gully erosion susceptibility assessment. Remote Sens 12:3620
545 Cook A, Merwade V (2009) Effect of topographic data, geometric configuration and modeling approach
546 on flood inundation mapping. J Hydrol 377:131–142
547 Costache R (2019) Flash-flood Potential Index mapping using weights of evidence, decision Trees
548 models and their novel hybrid integration. Stoch Environ Res Risk Assess 33:1375–1402
549 Costache R, Arabameri A, Blaschke T, et al (2021) Flash-Flood Potential Mapping Using Deep Learning,
550 Alternating Decision Trees and Data Provided by Remote Sensing Sensors. Sensors 21:280.
551 https://doi.org/10.3390/s21010280

552 Costache R, Bui DT (2020) Identification of areas prone to flash-flood phenomena using multiple-criteria
553 decision-making, bivariate statistics, machine learning and their ensembles. Sci Total Environ
554 712:136492
555 Darabi H, Choubin B, Rahmati O, et al (2019) Urban flood risk mapping using the GARP and QUEST
556 models: A comparative study of machine learning techniques. J Hydrol 569:142–154
557 Delkash M, Al-Faraj FAM, Scholz M (2014) Comparing the export coefficient approach with the soil and
558 water assessment tool to predict phosphorous pollution: the Kan watershed case study. Water, Air,
559 Soil Pollut 225:2122
560 El-Magd SAA, Pradhan B, Alamri A (2021) Machine learning algorithm for flash flood prediction
561 mapping in Wadi El-Laqeita and surroundings, Central Eastern Desert, Egypt. Arab J Geosci 14:1–
562 14
563 Frattini P, Crosta G, Carrara A (2010) Techniques for evaluating the performance of landslide
564 susceptibility models. Eng Geol 111:62–72
565 Heidari A (2014) Flood vulnerability of the K arun R iver S ystem and short-term mitigation measures. J
566 flood risk Manag 7:65–80
567 Hill J, Linero A, Murray J (2020) Bayesian additive regression trees: A review and look forward. Annu
568 Rev Stat Its Appl 7:251–278
569 Hong H, Panahi M, Shirzadi A, et al (2018) Flood susceptibility assessment in Hengfeng area coupling
570 adaptive neuro-fuzzy inference system with genetic algorithm and differential evolution. Sci Total
571 Environ 621:1124–1141
572 Hooshyaripor F, Faraji-Ashkavar S, Koohyian F, et al (2020) Annual flood damage influenced by El Niño
573 in the Kan River basin, Iran. Nat Hazards Earth Syst Sci 20:2739–2751
574 Hosseini FS, Choubin B, Mosavi A, et al (2020) Flash-flood hazard assessment using ensembles and
575 Bayesian-based machine learning models: application of the simulated annealing feature selection
576 method. Sci Total Environ 711:135161
577 Islam ARMT, Talukdar S, Mahato S, et al (2021) Flood susceptibility modelling using advanced

578 ensemble machine learning models. Geosci Front 12:101075
579 Janizadeh S, Avand M, Jaafari A, et al (2019) Prediction Success of Machine Learning Methods for Flash
580 Flood Susceptibility Mapping in the Tafresh Watershed, Iran. Sustainability 11:5426
581 Kalantar B, Ueda N, Saeidi V, et al (2021) Deep Neural Network Utilizing Remote Sensing Datasets for
582 Flood Hazard Susceptibility Mapping in Brisbane, Australia. Remote Sens 13:2638
583 Kapelner A, Bleich J (2013) bartMachine: Machine learning with Bayesian additive regression trees.
584 arXiv Prepr arXiv13122171
585 Khosravi K, Pham BT, Chapi K, et al (2018) A comparative assessment of decision trees algorithms for
586 flash flood susceptibility modeling at Haraz watershed, northern Iran. Sci Total Environ 627:744–
587 755
588 Khosravi K, Pourghasemi HR, Chapi K, Bahri M (2016) Flash flood susceptibility analysis and its
589 mapping using different bivariate models in Iran: a comparison between Shannon's entropy,
590 statistical index, and weighting factor models. Environ Monit Assess 188:656
591 Khosravi K, Shahabi H, Pham BT, et al (2019) A comparative assessment of flood susceptibility
592 modeling using Multi-Criteria Decision-Making Analysis and Machine Learning Methods. J Hydrol
593 573:311–323
594 Liaw A, Wiener M, others (2002) Classification and regression by randomForest. R news 2:18–22
595 Liu R, Chen Y, Wu J, et al (2016) Assessing spatial likelihood of flooding hazard using na{\"\i}ve Bayes
596 and GIS: a case study in Bowen Basin, Australia. Stoch Environ Res risk Assess 30:1575–1590
597 Mahmoud SH, Gan TY (2018) Multi-criteria approach to develop flood susceptibility maps in arid
598 regions of Middle East. J Clean Prod 196:216–229
599 Miles J (2014) Tolerance and variance inflation factor. Wiley StatsRef Stat Ref Online
600 Molinos-Senante M, Hernández-Sancho F, Sala-Garrido R (2011) Cost--benefit analysis of water-reuse
601 projects for environmental purposes: A case study for Spanish wastewater treatment plants. J
602 Environ Manage 92:3091–3097
603 Ngo P-T, Hoang N-D, Pradhan B, et al (2018) A Novel Hybrid Swarm Optimized Multilayer Neural

604 Network for Spatial Prediction of Flash Floods in Tropical Areas Using Sentinel-1 SAR Imagery
605 and Geospatial Data. Sensors 18:3704. https://doi.org/10.3390/s18113704
606 Panahi M, Dodangeh E, Rezaie F, et al (2021) Flood spatial prediction modeling using a hybrid of meta-
607 optimization and support vector regression modeling. Catena 199:105114
608 Papaioannou G, Vasiliades L, Loukas A (2015) Multi-criteria analysis framework for potential flood
609 prone areas mapping. Water Resour Manag 29:399–418
610 Pham BT, Avand M, Janizadeh S, et al (2020a) GIS Based Hybrid Computational Approaches for Flash
611 Flood Susceptibility Assessment. Water 12:683
612 Pham BT, Phong T Van, Nguyen HD, et al (2020b) A Comparative Study of Kernel Logistic Regression,
613 Radial Basis Function Classifier, Multinomial Na{\"\i}ve Bayes, and Logistic Model Tree for Flash
614 Flood Susceptibility Mapping. Water 12:239
615 Plant E, King R, Kath J (2021) Statistical comparison of additive regression tree methods on ecological
616 grassland data. Ecol Inform 61:101198
617 Prado EB, Moral RA, Parnell AC (2021) Bayesian additive regression trees with model trees. Stat
618 Comput 31:1–13
619 Prasad P, Loveson VJ, Das B, Kotha M (2021) Novel Ensemble Machine Learning Models in Flood
620 Susceptibility Mapping. Geocarto Int 1–22. https://doi.org/10.1080/10106049.2021.1892209
621 Pratola MT, Higdon DM (2016) Bayesian additive regression tree calibration of complex high-
622 dimensional computer models. Technometrics 58:166–179
623 Rahmati O, Pourghasemi HR, Zeinivand H (2016) Flood susceptibility mapping using frequency ratio and
624 weights-of-evidence models in the Golastan Province, Iran. Geocarto Int 31:42–70
625 Rish I, others (2001) An empirical study of the naive Bayes classifier. In: IJCAI 2001 workshop on
626 empirical methods in artificial intelligence. pp 41–46
627 Shafapour Tehrany M, Shabani F, Neamah Jebur M, et al (2017) GIS-based spatial prediction of flood
628 prone areas using standalone frequency ratio, logistic regression, weight of evidence and their
629 ensemble techniques. Geomatics, Nat Hazards Risk 8:1538–1561

630 Shafizadeh-Moghadam H, Valavi R, Shahabi H, et al (2018) Novel forecasting approaches using
631 combination of machine learning and statistical models for flood susceptibility mapping. J Environ
632 Manage 217:1–11
633 Shahabi H, Shirzadi A, Ghaderi K, et al (2020) Flood detection and susceptibility mapping using sentinel-
634 1 remote sensing data and a machine learning approach: Hybrid intelligence of bagging ensemble
635 based on k-nearest neighbor classifier. Remote Sens 12:266
636 Sparapani R, Spanbauer C, McCulloch R (2021) Nonparametric machine learning and efficient
637 computation with bayesian additive regression trees: the BART R package. J Stat Softw 97:1–66
638 Sparapani RA, Logan BR, McCulloch RE, Laud PW (2016) Nonparametric survival analysis using
639 Bayesian additive regression trees (BART). Stat Med 35:2741–2753
640 Talukdar S, Ghose B, Salam R, et al (2020) Flood susceptibility modeling in Teesta River basin,
641 Bangladesh using novel ensembles of bagging algorithms. Stoch Environ Res Risk Assess 34:2277–
642 2300
643 Tang X, Li J, Liu M, et al (2020) Flood susceptibility assessment based on a novel random Na{\"\i}ve
644 Bayes method: A comparison between different factor discretization methods. Catena 190:104536
645 Tang Z, Yi S, Wang C, Xiao Y (2018) Incorporating probabilistic approach into local multi-criteria
646 decision analysis for flood susceptibility assessment. Stoch Environ Res risk Assess 32:701–714
647 Tehrany MS, Jones S, Shabani F (2019a) Identifying the essential flood conditioning factors for flood
648 prone area mapping using machine learning techniques. Catena 175:174–192
649 Tehrany MS, Kumar L (2018) The application of a Dempster--Shafer-based evidential belief function in
650 flood susceptibility mapping and comparison with frequency ratio and logistic regression methods.
651 Environ Earth Sci 77:490
652 Tehrany MS, Kumar L, Shabani F (2019b) A novel GIS-based ensemble technique for flood
653 susceptibility mapping using evidential belief function and support vector machine: Brisbane,
654 Australia. PeerJ 7:e7653
655 Tehrany MS, Pradhan B, Jebur MN (2014) Flood susceptibility mapping using a novel ensemble weights-

656 of-evidence and support vector machine models in GIS. J Hydrol 512:332–343
657 Tehrany MS, Pradhan B, Mansor S, Ahmad N (2015) Flood susceptibility assessment using GIS-based
658 support vector machine model with different kernel types. Catena 125:91–101
659 Vafakhah M, Loor SMH, Pourghasemi H, Katebikord A (2020) Comparing performance of random forest
660 and adaptive neuro-fuzzy inference system data mining models for flood susceptibility mapping.
661 Arab J Geosci 13:417
662 Vetrivel A, Gerke M, Kerle N, et al (2018) Disaster damage detection through synergistic use of deep
663 learning and 3D point cloud features derived from very high resolution oblique aerial images, and
664 multiple-kernel-learning. ISPRS J Photogramm Remote Sens 140:45–59
665 Woodward M, Kapelan Z, Gouldby B (2014) Adaptive flood risk management under climate change
666 uncertainty using real options and optimization. Risk Anal 34:75–92
667 Wu W, Tang X, Lv J, et al (2021) Potential of Bayesian additive regression trees for predicting daily
668 global and diffuse solar radiation in arid and humid areas. Renew Energy
669 Yariyan P, Janizadeh S, Van Phong T, et al (2020) Improvement of Best First Decision Trees Using
670 Bagging and Dagging Ensembles for Flood Probability Mapping. Water Resour Manag 1–17
671 Yesilnacar E, Topal T (2005) Landslide susceptibility mapping: a comparison of logistic regression and
672 neural networks methods in a medium scale study, Hendek region (Turkey). Eng Geol 79:251–266
673 Zhang H (2004) The Optimality of Naive Bayes, 2004. Am Assoc Artif Intell (www aaai org)
674 Zhao G, Pang B, Xu Z, et al (2019) Assessment of urban flood susceptibility using semi-supervised
675 machine learning model. Sci Total Environ 659:940–949
676